



Recent Advancements in EEG Signal Acquisition and Processing Techniques: A Review

Anurag Verma¹, Dr. Laxman Singh², M. Hari³

Faculty of Engineering, Dayalbagh Educational Institute, Agra, India¹

Noida Institute of Engineering & Technology, Gr. Noida, India^{2&3}

Abstract: This paper discusses the recent developments in EEG signal acquisition and processing for the detection of various neurological disorders like Epileptic Seizure, Stroke, tetraplegia and Alzheimer etc. Meanwhile a brief study is also made with MEG signal processing as the future detection method. This paper also discusses integration of EEG with other neuroimaging techniques like ECG, NIRS, and FEM.

Keywords: Electroencephalogram (EEG), ECG, NIRS, FEM and Magnetoencephalography (MEG).

I. INTRODUCTION

A. Electroencephalogram Basics

EEG is the recording of bio-electric potentials generated by neurons in the human brain, which is mostly measured by many electrodes attached to the human scalp with the help of water-based conductive gel. EEG is the widely used non-invasive brain imaging technique [1]. EEG is a method to represent a form of the energy coming from particular points of the human scalp. An EEG also represents mental states and their variations. An instance of EEG representation of a mental state is the Contingent Negative Variation voltage which represents a mental state of prediction. Another instance is the value of an EEG alpha wave. The alpha wave is the major EEG pattern of a person who is awake and relaxed with eyes closed [2].

Biopotential measurement from the head shows the bioelectric role of the brain. This measurement is known as EEG. The first recording of EEG was done by the Austrian psychiatrist Dr. Hans Berger in 1929 by using a basic galvanometer and electrodes placed on his son's head; he showed the EEG as rhythmic waves of electrical oscillations. The EEG is generated by electrical dipoles in the outer brain cortex. The electric signal is believed to be reducible to the aggregate of excitatory and inhibitory postsynaptic potentials.

EEG waves are normally of 1 to 50 μV in magnitude with frequencies of 2Hertz to 50 Hertz. During neurological disorders like epileptic seizures, the EEG magnitudes can be as large as 1000 μV . Spectral study of EEG indicates certain peaks. Study of the EEG shows that these waveforms can be attached with some mental states. From awake to deep sleep, there is a rise of EEG activity, slowing from beta wave (around 18 Hz) to theta-delta wave (3.5 to 8 Hz). Fig. 1 shows the major brain wave frequencies.

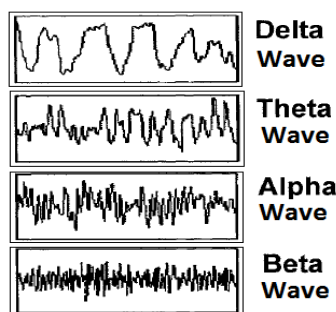


Fig. 1. Waveform appearances of four brain rhythms [3]

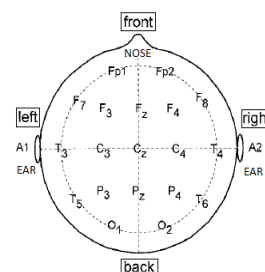


Fig. 2 The 10-20 lead system for placing EEG electrodes [3]

Generally EEG is used in the analysis of sleep patterns, the different stages of sleep, and the effects of different medicines on sleep. Mainly EEG is used in the analysis of epilepsy detection and diagnostic uses that find to decide epileptic seizure onset. The clinical EEG is normally analyzed using silver-silver chloride electrodes fixed to the scalp in a particular manner known as the 10-20 lead system shown in Fig. 2. This lead system gets its name from the reason that electrodes are placed at either 10 or 20% of the distances from markers on the scalp. EEG electrodes are normally used in differential pairs for higher



sensitivity to bio-electric potentials between a particular pair of electrodes. The alpha wave is strongest in the occipital lobe, whereas the beta wave is greatest in the frontal lobe [3].

B. EEG for Epileptic Seizure, Stroke and Alzheimer

Epilepsy is a common neurological disorder and it affects about 2% people in the world. Epilepsy is associated with events of sudden motor movements. These strange motor movements are because of hyper-synchronous discharges inside the human brain, and they are known as epileptic seizures. EEG is commonly used for detecting epileptic seizures. World Health Organisation has estimated that around 80 % of the epilepsy cases can be cured if a suitable diagnosis is performed at the earlier stage [4].

Presently there are different neuroimaging methods available for detection of epilepsy like electroencephalography (EEG). Different types of EEG tests are available from conventional EEG with different types of electrodes to many channel intra-cortical EEG. Unfortunately, many medical professionals lack the knowledge of separating epileptic seizures from other neurological disorders like psychogenic un-epileptic attacks and convulsive scope [5]. Around 50 million patients are already suffering from epilepsy. Cases of motor movements with fits (seizures) are common in epilepsy. These sensory movements are due to sudden electrical discharges of different electrical signals in the human brain. Among various detection techniques, EEG is most commonly preferred method [6]. Epilepsy is a chronic neurological disease after Alzheimer's and stroke. The major cause of Epileptic seizure is a disproportionate activity of large groups of neurons in the human brain. The epileptic disease leads to variety of short duration changes in cognition and psychological behaviour. Also, Epileptic patients always have mental stress and anxiety that associates random seizure attacks [7].

To stop the progress of rising older population with Alzheimer's disease, a new diagnosis method called neuronal activity topography system is developed that consists of a 21-channel EEG system connected to a remote computer through the internet. The EEG waves are affected by a condition of Alzheimer's disease and anomalies of the EEG. Some researchers tried to find useful information involved in EEG signals of Alzheimer's disease patients [8]. Epilepsy is a serious neurological syndrome characterised by sudden debilitating seizures that can cause harm to the person, affecting their quality of life, and may also lead to untimely death. Except for its high occurrence and serious problems, wrong diagnosis of 25% of people has been reported. An EEG plot of the brain's electrical activity is often required for sure detection of epilepsy. Although, seizures may happen within a span of few hours, weeks, or months, and so, long-term EEG plots may be needed to

record the brain electrical potentials during a seizure [9]. The EEG plots are often inspected by neurophysiologists to detect the seizures. Furthermore, the EEG plots are subjected to disturbances from noise, artefacts and interfering expressions. Therefore, visual inspection of the epileptic activity from EEG plots proves to be very long and difficult even for an experienced doctor. Developing countries have reported about 80% of epilepsy incidences. Due to this procedure for automatic detection of Epilepsy can help as a basic clinical method for the scrutiny of EEG plots in a more robust, accurate and efficient way [10]. Noise contaminates conventional scalp EEG represented by non-brain electrical activity such as ocular artefacts, scalp muscle potentials, and ECG. Additional noise is sometimes produced by very high electrode impedance, electrode displacements, amplifier drifts, etc. The noise can be larger than, the brain potential of interest and poses a major problem for neurologists [11]. When an artery carrying blood from heart to the brain bursts or a clot stops the blood flow the stroke occurs and reduces delivery of oxygen and nutrients. Moreover, ischemic stroke is the main reason of morbidity and long duration disability across the globe, and is among the main causes of death. Stroke accounts for nearly 10% of deaths and about 5% of health-care costs. In India, stroke cases in youths are high (18-32% of all stroke cases).

Quantitative EEG study has been used for identifying subclinical brain injury during neurosurgical procedures and it is also used for ischemia detection, global function assessment, medication titration, and prognostication. Moreover high, multilevel reproducibility has been shown in EEG parameters are reliably differentiated between stroke and transient ischemic attack (TIA) patients or control subjects, and correlated mostly with clinical and radiological status. Reliable EEG analysis is performed in a normal stroke population for medically relevant state and output measures [12].

II. RECENT TECHNIQUES IN EEG SIGNAL ACQUISITION

A. Cross-layer design of Energy Minimization

Here wireless EEG monitoring system is considered as shown in Fig. 3. We are mainly concerned with data collection procedure from the low-power sensor points to the coordinator. Each sensor node is small; battery powered and required to run ideally for days by using a transmitter and a receiver antenna. The work here uses encoding model for EEG data and it can be extended to a range of vital signatures which are at a lower data rate like temperature, pressure or heart beats, or at higher data rate such as of ECG signals. We use Time Division Multiple Access which removes disturbance. At the MAC level, the coordinator finds the decided sensor point and the fixed slots length, according to the user needs and the channel condition to reduce the energy use. Figure 4 shows the



structure of the EEG encoder. The main blocks considered are amplifier and sampler, Discrete Wavelet Transform, quantization and encoding of the DWT coefficients

reduction of various artefacts, by 100 dB at one radius from the electrode [11].

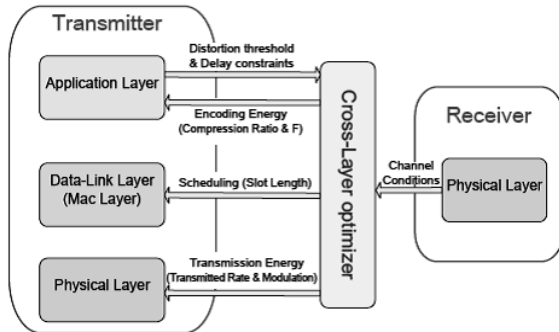


Fig. 3 Cross-layer design of Energy Minimization [13].

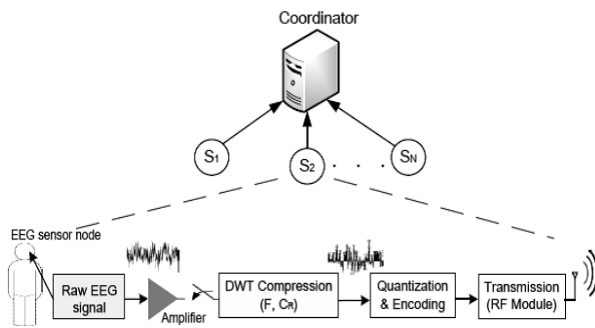


Fig. 4 The model of EEG Encoder [13].

B. EEG with Using Tripolar Concentric Ring Electrodes

The tripolar concentric ring electrode, a new electrode structure, is used to avoid the poor SNR and reference defects of the disc electrodes. This configuration consists of three electrodes - outer ring, middle ring, and the central ring as shown in fig. 5 for recording electrical signals from the brain by its three closely placed rings. It is very different from the conventional disc electrode with a single ring. It can give three signals from the three electrode rings for recording two differential signals for the tripolar Laplacian derivation described as; weighted sum = {16*(M-D)-(O-D)};

Where O, M, and D are the potentials on the outer ring, middle ring, and central disc. The tripolar concentric ring electrode (TCRE) performs the Laplacian derivation automatically and takes bipolar differentials of the surface potentials from closely spaced concentric electrode ring at around 1mm space in between with preamplifier as a differential amplifier. With the electrode rings placed at 1mm space in between, artefacts like eye blinks, muscle or motion contribute equally and are cancelled when bipolar differentials are done by the preamplifier. EEG recorded with the TCRE has about 374% increase in SNR and 8.27% the mutual interference between signals recorded from two adjacent TCREs. The TCRE has a strong

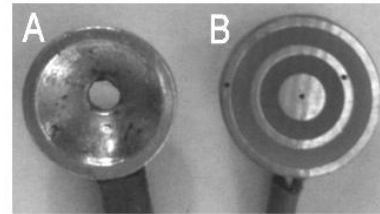


Fig. 5 Configurations for EEG electrodes: A-Conventional electrode, B- Tripolar concentric ring electrode [11].

C. Automatic Diagnosis of Epilepsy

The signal processing methods for automatic diagnosis of epilepsy like the linear prediction model based energy of EEG signals is explored for the classification of epileptic seizures. This method uses the time-domain characteristics like spikes and magnitude of the signal for epileptic seizure detection using EEG. Automated detection of epileptic seizure is done in fractional calculus based linear prediction method with error energy and energy computations of EEG signals along with support vector machine. For classification of normal and epileptic seizure EEG plots, artificial neural network classifier is used. The ANN classifier is used with principal component analysis based method for classification of epileptic seizure for detection of epilepsy. In another research, wavelet transform for getting sub-bands of EEG signals and several statistical characteristics of these sub-bands are calculated. The modified forms of generalised fractal dimensions and DWT based method had been utilized for epileptic seizure diagnosis. The new method shown in figure 6 for automatic detection of epilepsy uses the calculation of LBP only at a set of stable key-points, which are found through a multi-scale study of the EEG signal. The new method gives significant enhancement in performance because of increased differentiating ability of the LBP based classifier when calculated at key points [14].

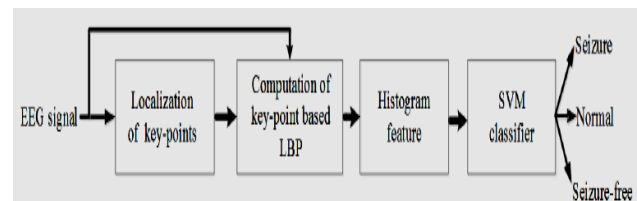


Fig. 6 Block diagram for Automatic Diagnosis of Epilepsy [14].

D. EEG Source Imaging

For the people suffering from acute neurological injury, brain-computer interface (BCI) technology has given an alternative means of communication with the environment outside of the body. The sensory motor rhythm (SMR)



is an oscillatory idle brain wave of synchronised electric brain activity. It appears in spindles during recordings of EEG, MEG, and ECoG over the sensory motor cortex. For most people the frequency of the SMR is in the range of 13 to 15 Hz. SMR-based BCIs have got control of both imaginary and real objects up to three dimensions. Control signals taken for SMR BCIs are found on the voluntary modulation of frequency-specific electrical activity. In short, the following points are needed to be taken care of for SMR BCIs to improve for everyday uses are:

- 1) The lesser spatial resolution of EEG broadly restricts the number of MI jobs that can be used to control SMR BCI.
- 2) MI jobs that generate unique and usable control signals are not matched to the action of the output device and make it tough to give neuro-feedback reflective of the user's intention. MI tasks involve four different jobs of the right hand: flexion, extension, supination, and pronation as shown in figure-7. These jobs were chosen to represent complex actions used in the fine motor control of the hand which could be applied to both rehabilitative and prosthetic control uses. It is greatly improved the differentiation of these tasks by using a source-based method beyond the peak accuracy achieved by the sensor-based approach [15].

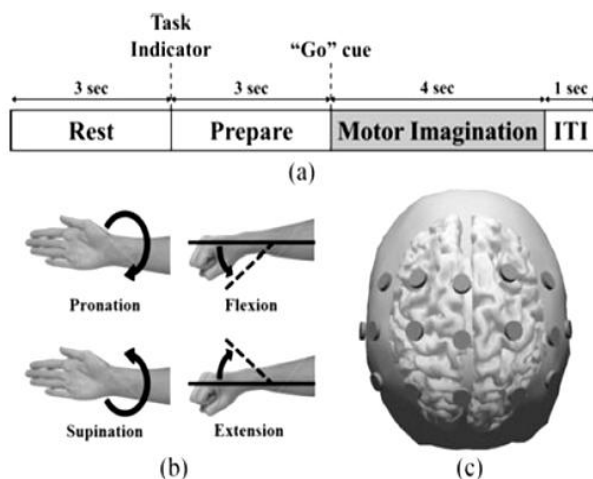


Fig.-7 Different MI Jobs for EEG Source Imaging [15]

III. MEG SIGNAL PROCESSING

MEG is a neuro physiological analysis method that uses a superconducting quantum interference device (SQUID) for acquiring brain's electrical signals. Spikes and sharp waves present in MEG signals can be used to diagnose epilepsy. MEG spikes are more easily differentiable compared to EEG peaks and seem to be sharper. The MEG signals have the nature of multi channel variables. The most common method for detecting peaks from brain signals is by visual inspection of plots. Manually finding the epileptic peaks in MEG plots is very tedious and time

consuming. The high density of MEG sensors gives a good presentation of the magnetic field distribution over the scalp. However, the high number of MEG sensors (300) makes visual inspection time taking, as it is impossible to show and analyze so many channels together. Also the visual inspection is a subjective method, which can lead to arguments among neurologists analyzing the same data. So automatic diagnosis of epileptic peaks, based on objective criteria, would be useful for quantitative study and medical diagnosis. The proposed algorithm has features extractor and classifier, carefully selected for the inherent properties of MEG signals. This study shows that:

- 1) The common spatial patterns can be used to find differentiating features from MEG spikes which, unlike EEG plots, do not have fixed morphological features.
- 2) The CSP features extracted from the MEG data reasonably follow a normal distribution. Hence linear discriminated analysis (LDA) can be used for classification; CSP method gets spatial filters that can be used for the differentiation between two categories of signals. The obtained filters must ensure maxima of the variance of one category of signals and minima of the other category. LDA is a simple and robust categorization method which looks for a linear set of predictors that best differentiates different categories. The spike detection method achieves 91.03% sensitivity and 94.21% specivity; hence it is a valuable technique for neurologists handling with MEG data for medical diagnosis [16].

VI. STATE OF THE ART TECHNIQUES IN EEG SIGNAL PROCESSING

A. Automated Detection of generalised seizures using 3D Phase Trajectory

1) Data Source:

The data source is online data from the database of University of Bonn, Germany. The EEG signals in this data have five sub sets. Sets Z and O are taken from normal people when eyes were open and closed. Sets N and F were taken from epilepsy people during the time of non-seizure condition from their epileptogenic zone and hippo campus of the opposite hemisphere. Signals in online data are taken with sampling frequency of 173.61 Hz

2) Feature extraction:

2.1 Signal decomposition into intrinsic mode functions
The intrinsic mode functions (IMFs) shows the amplitude and frequency modulated symmetric parts of the signals. These are taken by application empirical mode decomposition (EMD) on signals. Here Hilbert Transform is used which provides the multi-scale study of nonlinearities in the signals. Use of EMD has been realised in analysing centre of pressure, electrocardiogram, electromyogram (EMG), and various biomedical uses. The



IMFs from signals $x(t)$ are taken via a shifting iterative method as follows:

- Calculation of maximum and minimum points of signal $x(t)$.
- Fitting the extrema using cubic spline interpolation. This generates envelopes $e_m(t)$ and $e_n(t)$ where m and n are natural numbers.
- Calculation of local mean $l(t)$ of created $e_m(t)$ and $e_n(t)$ envelopes
- Extraction of detail given by $d_1(t) = x(t) - l(t)$.
- These steps are repeated till the conditions for IMFs are fulfilled.

The necessary conditions for IMFs are:

- The number of maximum and minimum points must be ≤ 1 .
- The mean of two envelopes made by the above method should be equal to zero.

Let the first IMF of the signal be $IMF_1(t)$. This is given by $IMF_1(t) = d_1(t)$. Remaining IMFs are calculated by

$$r_1(t) = x(t) - IMF_1(t) \quad \dots(1)$$

Where $r_1(t)$ is the residue. The value of $r_M(t)$ thus obtained does not satisfy the necessary conditions for IMFs therefore, serves as the termination criteria of the iterative process. The original signal $x(t)$ may be reconstructed by the following equation:

$$x(t) = \sum_{m=1}^M IMF_m(t) + r_M(t) \quad \dots(2)$$

Now, for each IMF, different value of local frequency is obtained. Therefore, the equation (2) can be rewritten as

$$x(t) \approx \sum_{m=1}^M A_m(t) + \cos\{\phi_M(t)\} \quad \dots(3)$$

Where $A(t)$ and $\phi(t)$ are the amplitude and phase of a signal. The starting nine IMFs generated from each of the input signals were used to represent 3D phase trajectories in this analysis.

2.2 Representation of 3D phase trajectories

A non-stationary signal (Here EEG) is analysed by its state and dynamics. These features evolved over the traces of time may be visually reported by paths called phase space trajectories. Let V indicates the vectors of EEG signal $x(t)$ in time series. The phase trajectories T can be written as:

$$T_n = \{V_n, V_{n+\tau}, \dots, V_{n+(d-1)\tau}\} \quad \dots(4)$$

where, $n= 1,2,\dots,N-(d-1)\tau$ is the number of data points, d is the dimension of pointing the phase trajectories, τ is the time lag. The phase trajectories can be represented over multi-dimensions by changing the value of d . For the ease of representation, we have kept $d = 3$ and $\tau = 1$. Fig. 8 shows the 3D phase trajectories for

starting four IMFs of a seizure-free EEG signal from the data sets. Fig. 9 shows the 3D phase trajectories for starting four IMFs of an EEG signal with seizure movements taken from the data sets. Because separating the seizure and non-seizure signals by looking at their 3D phase trajectories is very difficult, therefore, it is required to automate this procedure. Therefore, average values of Euclidean displacements from ellipse patterns are calculated.

2.3 Calculation of mean Euclidean distances

The Euclidean distances between the three delayed vectors V_n, V_{n+1} and V_{n+2} are calculated and their average was taken using the equations:

$$E_n = \sqrt{V_n^2 + V_{n+1}^2 + V_{n+2}^2} \quad \dots(5)$$

$$\mu_n = \sum_{n=1}^N E_n \quad \dots(6)$$

The average values of the Euclidean distances are taken as the input feature vectors for the classification process.

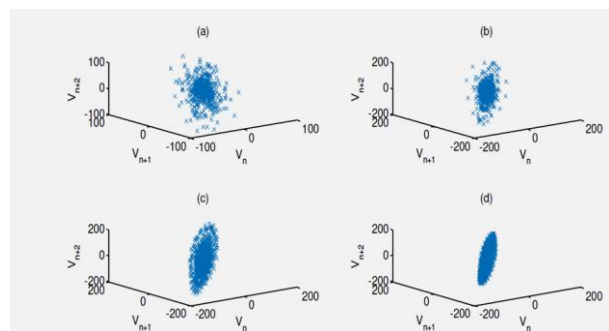


Fig.8-3D phase trajectories for IMF1-4 of a seizure-free EEG signal [6].

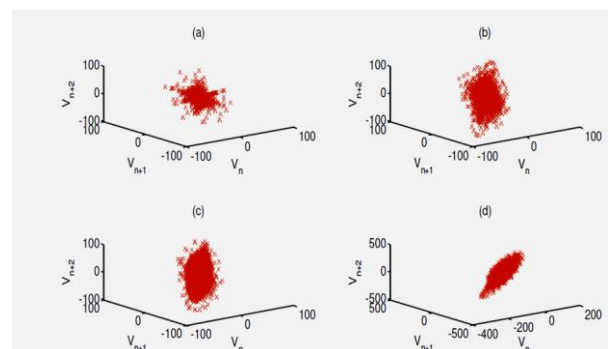


Fig.9-3D phase trajectories for IMF1-4 of a seizure EEG signal [6].

3. Probabilistic neural network classifier:

The architecture of PNN is given in Fig. 10. It has three layers.

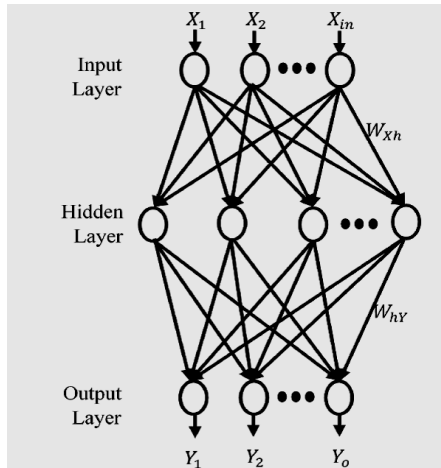


Fig.10- Probabilistic neural network (PNN) Architecture [6].

The first layer scales the input vectors by subtracting the median values and dividing by the interquartile ranges. The second layer is the hidden layer which calculates the class having maximum probability density function (PDF). The final third layer has summation units which separate the vectors depending upon their PDFs. This method uses Bayesian process to find the optimal solution. Unlike back-propagation neural networks PNN does not need to be trained again and again. Therefore because of high computation speed, it is best for practical applications. The outputs were calculated using following equations:

$$net_0 = \frac{1}{N_0} \sum_h W_{hY} H_h \quad \dots (7)$$

$$C_0 = \sum_h W_{hY} \quad \dots (8)$$

If $net_0 = \max_k(net_k)$ then, $y_0=1$ else, $y_0=0$;

in are the input layers

h are the hidden layers

o are the output layers

k are training sets

C are classification sets

X are input vectors

W_{Xh} are weights between input layer X and hidden layer H

W_{hY} are weights between hidden layer H and input layer X. G-fold cross-validation verifies the results. The value of G is set to 10. Out of the ten sets, three sets are taken for testing the designed expert model and the remaining of the sets are used for training.

4. Performance parameters

The classification performance of the expert model is tested based on following parameters computed:

1) Classification accuracy (in %): It is the measure of the total accuracy of the model to correctly classify the test data.

- 2) Sensitivity (in %): It is a statistical measure of the model to accurately classify seizure patterns.
- 3) Specificity (in %): It is the statistical measure of the model to accurately classify seizure-free patterns.
- 4) Computation time (in s): It is the time elapsed for testing [6].

B. Multi-resolution analysis using dual-tree complex wavelet transforms (DTCWT)

1. Source datasets:

The data set is online data from the database of University of Bonn, Germany. The EEG signals in this data have five subsets as shown in fig. 11. Each subset in this database has the scalp recordings acquired at a sampling rate of 400 Hz. The acquisition is done using sixteen channels gold electrodes with the international 10–20 EEG electrode placement system. Data is further divided into two types, with each segment having 1200 epochs lasting for 10 seconds. The first type of the data has ictal signals. The second type of the data has background nonictal activities coming from the same person.

2. Multi-resolution analysis (MRA) using dual-tree complex wavelet transforms (DTCWT)

This architecture uses two real-valued discrete wavelet transforms (DWTs) as shown in fig.12. In complex wavelet transform the complex-valued wavelet is represented by-

$$\psi_c(t) = \psi_r(t) + j\psi_i(t) \quad \dots (9)$$

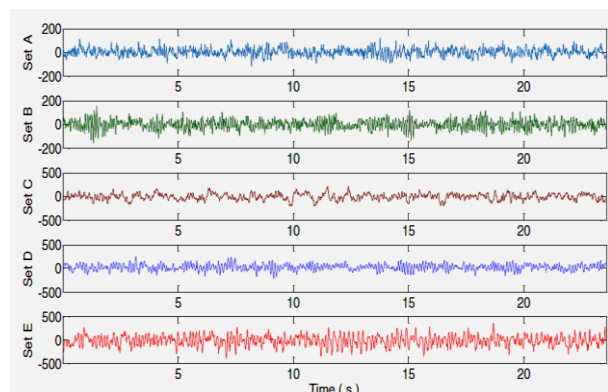


Fig.11-Online EEG database of University of Bonn [10].

In the above equation, $\psi_r(t)$ shows the real and even part of wavelet while, $j\psi_i(t)$ shows the imaginary and odd part of wavelet. The $\psi_r(t)$ is roughly the Hilbert transform represented by H of $\psi_i(t)$ i.e. equated as $\psi_r(t) \approx H\{\psi_i(t)\}$. Therefore, making $\psi_c(t)$ an analytic signal. Also the complex wavelet coefficient can be defined as follows:

$$d_c(j, k) = d_r(j, k) + jd_i(j, k) \quad \dots (10)$$

The value of magnitude and phase for the above equation are calculated by the following equations:



$$|d_c(j,k)| = \sqrt{[d_r(j,k)]^2 + [jd_i(j,k)]^2} \quad \dots (11)$$

$$\angle d_c(j,k) = \tan^{-1} \left[\frac{d_{i1}(j,k)}{d_r(j,k)} \right] \quad \dots (12)$$

When $|d_c(j,k)| > 0$. This helps coherent multi-resolution analysis of signals exploiting both the magnitude and phase information. The evaluation of $\psi_r(t)$ and $\psi_i(t)$ needs use of dual FB trees. Tree 1 is used to find the real part of the transform, and Tree 2 is used to calculate the imaginary part of the transform. The filter banks (FBs) for the use of DTCWT up to three levels of decomposition as shown in Fig. 12. The signals are sequentially given to the recursive series of filters. At every decomposition level, sub-bands are down sampled by a factor of 2.

3. Feature extraction parameters:

For further calculations the extracted wavelet coefficients are saved. Let m be the length of decomposition level for details and last approximation coefficients, where $m = 1$ to 7. The initial six values of m show the details and the last value of m (i.e.7) shows the final approximation. Because, the entire signal can be reproduced by summation of all details. Only last approximation, the balance approximations are not used in this study. For n segments of EEG signals, wavelet coefficients having all six details and last approximation are shown as ω_{mn} .

Various feature sets are tested using the following equations with the extracted wavelet coefficients:

$$\text{Energy Values (ERD}_{mn}) = \sum_{n=1}^K |\omega_{mn}|^2 \quad \dots (13)$$

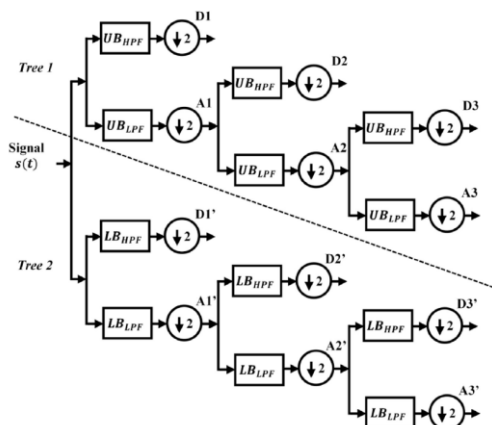


Fig.12- Architecture of DTCWT [10]

$$\text{RMS Values (RMS}_{mn}) = \sqrt{\frac{1}{K} \sum_{n=1}^K \omega_{mn}^2} \quad \dots (14)$$

$$\text{Mean Values } \mu_{mn} = \frac{1}{K} \sum_{n=1}^K \omega_{mn} \quad \dots (15)$$

Standard Deviation Values,

$$\text{STD}_{mn} = \sqrt{\frac{1}{K-1} \sum_{n=1}^K (\omega_{mn} - \mu_{mn})^2} \quad \dots (16)$$

Shanon Entropy Values,

$$\text{ENT}_{mn} = -\sum_{n=1}^K \omega_{mn}^2 \log(\omega_{mn}^2) \quad \dots (17)$$

$$\text{Maximum Peaks, } \text{MXP}_{mn} = \max(\omega_{mn}) \quad \dots (18)$$

Where K is the number of wavelet coefficients and the value of n depends on the combination of datasets taken. Out of all the characteristics in Eqs. (13) – (18), ERD and ENT are non-linear features. The neurons require high energy levels to sustain their normal working. The series of epileptic seizures creates unbalance in the physiological energy and entropy levels. Therefore ERD and ENT are taken for the current study. Also during seizure onset, the normal rhythmic activity of the brain gets disturbed and so the measure of statistical variations from normal state to epileptic state also form another set of features. Therefore RMS, MEAN and STD are taken as statistical features for the classification. It can be seen easily in Fig. 13 that the non-ictal and ictal features are overlapping in nature. This makes them very difficult and tedious to be accurately separated through visual inspection. Therefore a classifier is needed to separate these classes. For this target vectors y corresponding to the feature sets are prepared (labelled as ‘1’ for ictal activities and ‘2’ for non-ictal activities). Then the input data is separated into K number of folds and hence fed into the GRNN model for classification.

4. K-fold cross-validation:

K-fold cross-validation or rotation estimation is done in this study. The original dataset is separated into K sub-samples ($K=10$ here).

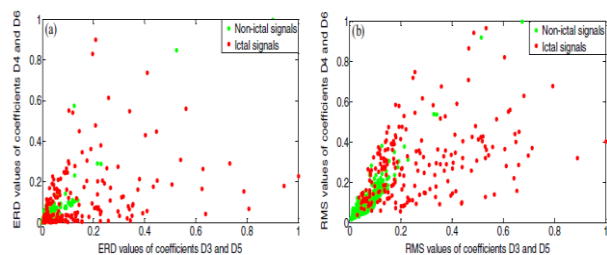


Fig.13-ERD and rms feature sets of non-ictal and ictal [10].

Out of these ten sub-samples, certain sub-samples (called the validation or testing sets) are saved as verification data for later testing of the model. In between the remaining sub-samples (the training sets) are taken for initial training of the model. It takes K times more computation time to



make a final evaluation. However, the tested computation timings still need to be verified for the speed of the classification.

5. General regression neural network (GRNN) classifier: An artificial intelligence based classifier has the mapping of a function f from r dimensional input feature space to q dimensional output space and it can be written as:

$f : R^r \rightarrow R^q$ (where, $q \leq r$). In ANN architecture, this mapping is achieved by simulating groups of artificial neurons depicting the human brain. The general regression neural network (GRNN) defines a memory-based network model that calculates the input variables and converges to the underlying regression surface. It forms one-pass learning with a highly parallel architecture. GRNN is not needed to be trained over the complete dataset and therefore, helps in quick up-gradation of the network with next patient's data. For uses in signal classification, the training sets in GRNN are classified according to their probability density function estimates. The architecture of GRNN model (as shown in Fig. 14) consists of four layers: The input layer: It is the distribution units which feed scaled measurements of variables X to all the neurons. The hidden layer: This layer consists of a neuron for each case of the training set. It calculates the Euclidean distance for the test case and then uses the radial basis function (RBF) kernel and the smoothing parameter (σ). The summation layer: It contains two neurons that serve as the denominator and numerator summation units. The decision or output layer: This layer divides the accumulated numerator summation unit by the denominator summation unit.

6. Evaluation of expert system's performance:

Following measures are considered to test the performance of the 10-fold GRNN classifier:

Sensitivity (SN): The measure of statistical performance of the expert system to accurately classify the seizure activities is calculated as follows:

$$SN = \frac{TP}{(TP + FN)} \times 100\% \quad \dots (19)$$

Specificity (SP): The measure of statistical performance of the expert system to correctly classify the normal activities is calculated as follows:

$$SP = \frac{TN}{(TN + FP)} \times 100\% \quad \dots (20)$$

Classification accuracy (CA): The measure of the proportion of samples correctly classified by the expert system out of the total test samples is calculated as follows:

$$CA = \frac{TP + TN}{(TN + TP + FN + FP)} \times 100\% \quad \dots (21)$$

Computation time (CT): It is the time taken for classification and is measured in seconds [10].

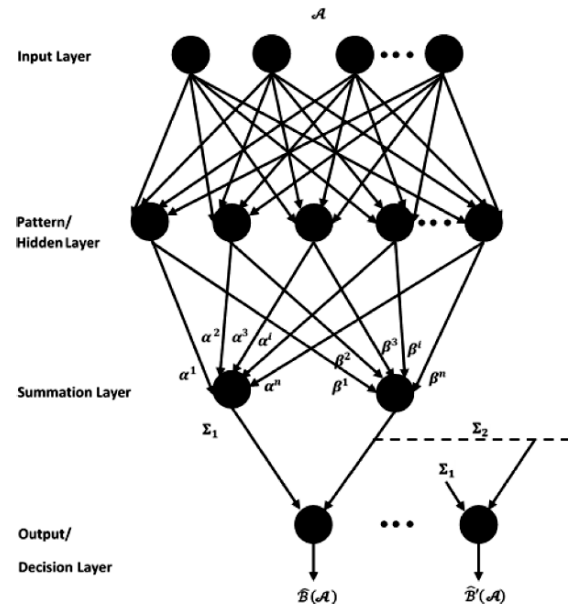


Fig.14-The general regression neural network (GRNN) Architecture [10]

V. COMBINATIONS OF EEG WITH OTHER NEURO-IMAGING TECHNIQUES

A. Quantification with Intracranial EEG and FEM Simulations

Endogenous modulation of neuronal activity through the ephaptic coupling at the cellular level has perceived rising attention in last few years. Many groups could show that the electric fields produced by active neurons feed back onto themselves. This ephaptic coupling is especially useful for natural electric fields. Electric fields of the order of magnitude of 0.2 V/m may be enough to elicit these effects. Transcranial electric stimulation (TES) also affects the electric field of the brain and shown to affect diverse brain functions, including present memory and learning functions, at similar cortical electric field strength as in the endogenous case. Except for neuronal activity, electrical muscle activity is another source of endogenous electric field. Strong muscle activity close to the brain happens when chewing-gum. Also this was shown that cognitive performance is improved after 15–20 minutes of chewing the gum. These skull defects can have a major impact on volume conduction that has to be taken care of. For this, we used detailed finite element method volume conductor head modelling calibrated with the patient data to calculate the strength of effects to be found in the lack of craniotomy defects, by closing the skull defects. Finally, an experiment is performed to determine the range of electromyogram strength during chewing of food with a variety of consistencies, including chewing gum. In short,



by this method, we arrived at quantitative predictions on the strength of chewing-related (ChR) cortical electric field to be expected in healthy people. Electro-cortico-gram (ECoG) and EEG (standard 10–20 positions) are together recorded at a sampling rate of 1024 Hz, along with high-pass filter of 1 Hz along with low-pass filter of 344 Hz. Measurements were taken during natural food intake of the patients without any prior information. Chewing events were marked manually within inter-ictal time periods based on both the digital video acquisition and on the typical, ChR EMG bursts of the masticator muscles visible in the EEG (in channels T4 and F8). EMG starting and end were pointed for every chewing event. To compare intra and extra cranial ChR EMG magnitudes, it is high-pass filtered at 100 Hz and, for every chew event, the ChR EMG magnitudes are calculated as the difference between the 10th and 90th percentile in a 100-ms time slot around the centre of each experiment. A volume conductor head model of subject S3 was used to model the extra- to intracranial conduction of electric potentials caused by bipolar sources located in the left temporal muscle. Subject S3 was selected since we had the best imaging data for making the FEM model. FEM calculations were calculated with SimBio as shown in figure-15. The conductivity values used were taken from the resistivity values used in white matter 0.14 S/m, gray matter 0.33 S/m, CSF 1.54 S/m, blood 0.63 S/m, skull 0.0063 S/m, muscle 0.11 S/m, soft tissue 0.17 S/m, and internal air 0.002 S/m. Foramina filled with both blood and nerves were modelled with 0.38 S/m, which is the average of both blood and white matter conductivities. Burr holes and saw lines, as found from CT data, were filled with CSF. For insulating silicone ECoG grid a conductivity of 1e-45 S/m was taken, which is the numerical conductivity closest to 0 S/m that SimBio could model [17].

C. Combined EEG-fNIRS Decoding

Motor-impaired people, such as tetraplegia patients, can benefit from the application of a brain-computer interface (BCI) which would enable them to control movements like a wheelchair or orthosis, driven by mental actions. Many BCIs are based on variations in sensorimotor waves: event-related de-synchronization (ERD) and synchronization (ERS), which can be detected in the EEG of an individual who is imagining or executing movements. The brain switch systems driven by motor jobs are based on electrophysiological signals; some studies have shown the feasibility of using functional near-infrared spectroscopy. Optical BCIs make use of concentration variations in the cerebral blood flow during increased neural activity, for example, motor jobs during which an increase of oxygenated haemoglobin (oxy-Hb) along with a fall in deoxygenated haemoglobin (deoxy-Hb) happens. There is a possibility of joining these hemodynamic responses with their electrophysiological counterparts, in a “hybrid” BCI as shown in figure-16. It

is tested that whether this principle works in patients with tetraplegia which is an important target group of brain switch techniques as follows.

1) EEG: After down-sampling the EEG data to 256 Hz and getting rid of the DC offset, linear de-trending was done to remove slow drifts. Visual analysis of the data showed class-specific data contamination in a very small number of turns and channels, which were excluded from further analysis. Spectral features were averaged over all subjects in order to calculate an average time-frequency plot showing the power decrease (ERD) while performing the movement jobs.

2) fNIRS: The optical signals from the fNIRS acquisition device were changed to haemoglobin changes using the modified Beer Lambert law. This changes the optical density variations to oxygenated and deoxygenated (HHb) concentration variations. The differential path length factor was taken individually for every subject according to their age. Slow drifts were taken off with a 0.01Hz high-pass filter. To improve the SNR, the concentration variations for the reference transmitter were scaled to fit the obtained concentration variations from the target transmitter with the least squares method. Subsequently, the scaled concentration changes of the reference transmitter were subtracted from the far transmitter. This was done to correct for systemic noise, including hemodynamic variations from scalp and skull, and was done for and HHb and both channels. Since actions faster than 0.2 Hz were not anticipated the concentration variations were low pass filtered to 0.2 Hz and are base-lined for every turn and channel to the period from 5 to 0 s before task start.

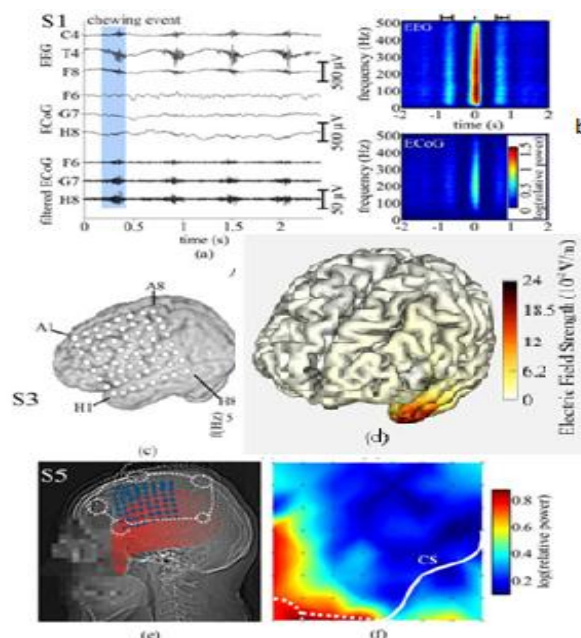


Fig.-15 Chewing related EEG and ECoG recordings



The filtered and HHb variations were taken as the features for classification [18]. Functional Near-Infrared Spectroscopy (fNIRS) is a noninvasive optical method that makes use of minimum two wavelengths in the near-infrared spectrum of light for the measurement of oxy (O₂Hb) and deoxy (HHb) haemoglobin concentration variations in cortical brain areas. Moreover, this ensures more robust methods for operation under real life situations. These improvements in wearable devices and BCI also affect new research areas attached to either domain: Neuro ergonomics and adaptive neuro technology research emphasise on the use of brain and body bio signals in the design of a complete human-machine interfaces. These interfaces have the potential to enhance work environments, efficiency and security and advancements of the understanding of brain function in real-world situations. For the hybrid neuro technology the joint acquisition of fNIRS and electrophysiological signals such as EEG, ECG or EMG, there are presently no appliances in the market and only very few are available in research. Although separate EEG and fNIRS tabletop instruments are commonly combined in stationary experiments, mobile situations need researchers to innovate their hybrid appliances. In this novel design for a new generation of customizable mobile, hybrid bio-optical/electrical designs that are capable with WBSN situations. By using a shared Analog Front-End and a powerful microcontroller, the above features are integrated with improved resolution (24 vs.: 16Bit in above devices), decreased costs and at the same time miniaturise way beyond the previous methods (4:2_4:2_0:6 cm3).

Although the design works for different types of signals and applications, present instrument is used in hybrid neuro-technology solutions, particularly BCI and neuro-ergonomics. Here the focus is on fNIRS and EEG signals, and aid within the same device ACCEL, ECG and EMG as extra modalities. In the present design, it is shown how to use functional parts from our open NIRS design to effectively create hybrid technology for the acquisition of both electrical and optical bio-signals. The present work does not deal with multimodal signal processing for parameter extraction or artefact suppression; this is left for future work.

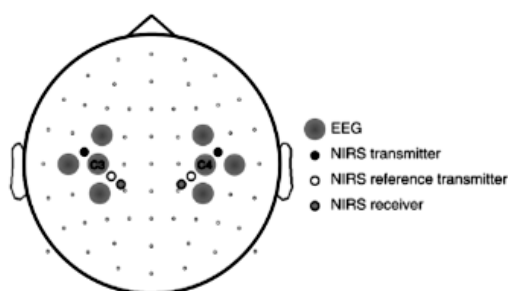


Fig. 16 Combined EEG-fNIRS Channel Configuration.

By sharing the architecture and corresponding characteristics here, we hope to facilitate future designs by researchers in related fields. To illustrate the system concept and scope of applications for the Mobile, Modular, Multimodal Bio signal Acquisition device, fig. 17 shows an exemplary hybrid WBSN BCI scenario [19].

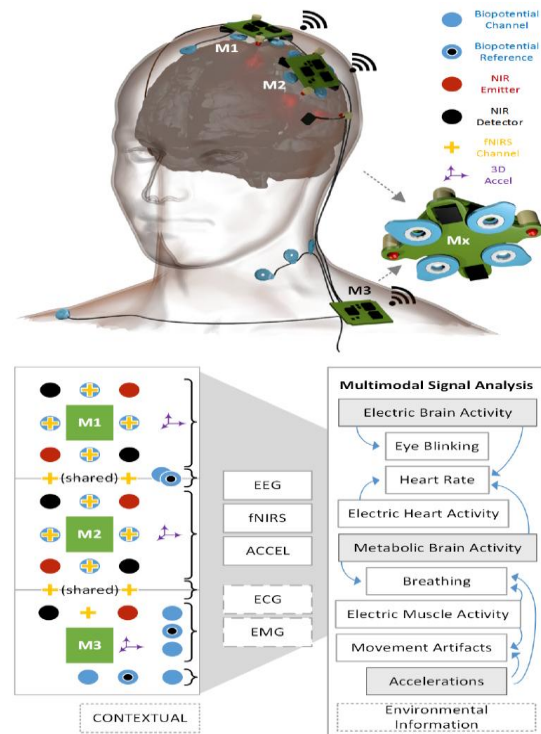


Fig. 17 Mobile, Modular, Multimodal Bio signal Acquisition System [19].

D. Smart helmet

A proof-of-concept study of the feasibility for EEG and ECG recordings from within a helmet is shown in figure-18, and this device is referred as the smart helmet.

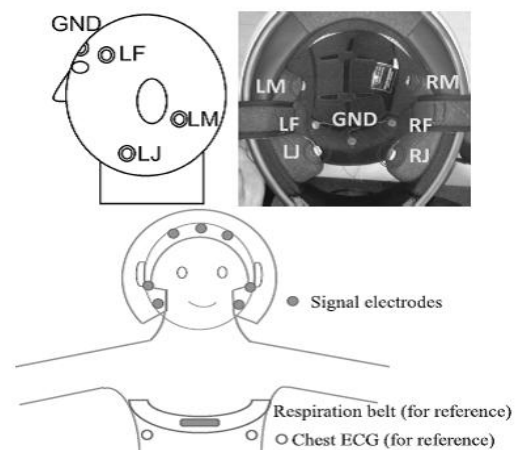


Fig. 18 Smart Helmet Configuration [20].



In combination with the physiological responses derived from ECG and EEG, such as respiration via respiratory sinus arrhythmia (RSA), EMG via accelerometers, movement, and temperature, this promises a feasible tool for examining the state of body and mind of a user wearing the smart helmet. More precisely, the two main aims of this work are: (i) to introduce a smart helmet which can record the ECG and EEG without a decrease in comfort or any inconvenience to the user and in real-world situations, therefore showing wearable nature; and (ii) to propose robust multivariate signal processing for the identification of R-peaks in noisy ECG and the diagnosis of EEG results. This method ensures a high accuracy even in noisy conditions [20].

VI. CONCLUSION

In this paper we discussed recent developments in EEG signal acquisition and processing for the automatic detection of various neurological disorders like Epileptic Seizure, Stroke, tetraplegia and Alzheimer etc. are discussed. In addition a brief study about MEG signal processing as the future detection method is also presented. Other neuro imaging techniques such as ECG, NIRS, and FEM integrated with EEG are also presented in this paper.

REFERENCES

- [1] S. Makeig, C. Kothe, T. Mullen, N. B. Shamlo, Z. Zhang, and K. K. Delgado, "Evolving Signal Processing for Brain-Computer Interfaces", proceedings of the IEEE, vol. 100, pp.1567-1584, 2012.
- [2] S. Bozinovski, and A. Bozinovski, "Mental States, EEG Manifestations, and Mentally Emulated Digital Circuits for Brain-Robot Interaction" IEEE Transactions on Autonomous Mental Development, Vol. 7, no. 1, pp. 39-51, March 2015.
- [3] M. Kutz, Biomedical Engineering and Design Handbook, 2009, The McGraw-Hill Companies, Inc.
- [4] P. Swami, M. Bhatia, T. Gandhi, B. K. Panigrahi and S. Anand," Locating Ictal Activities over Human Scalp with Automated Detection using EEG signals", proceedings of 3rd International Conference on Signal Processing and Integrated Networks (SPIN), pp. 600-604, February 2016.
- [5] P. Swami, T. K. Gandhi, B. K. Panigrahi, M. Bhatia J. Santhosh and S. Anand, "A comparative account of modelling seizure detection system using wavelet techniques", International Journal of Systems Science: Operations & Logistics, pp 1-12, January-2016.
- [6] P. Swami, T. K. Gandhi, B. K. Panigrahi, M. Bhatia, and S. Anand, "Detection of Ictal Patterns in Electroencephalogram Signals using 3D Phase Trajectories", proceedings of IEEE INDICON, pp 1-6, 2015.
- [7] S. Supriya, S. Siuly, H. Wang, J. Cao, and Y. Zhang, "Weighted Visibility Graph with Complex Network Features in the Detection of Epilepsy" special section on big data analytics for smart and connected health, IEEE Access, pp 6554-6566, October 2016.
- [8] T. Musha, H. Matsuzaki, Y. Kobayashi, Y. Okamoto, M. Tanaka, and T. Asada, "EEG Markers for Characterizing Anomalous Activities of Cerebral Neurons in NAT(Neuronal Activity Topography) Method", IEEE Transactions on Biomedical Engineering, vol. 60, no. 8, pp 2332-2338, August 2013.
- [9] S. A. Imtiaz, L. Logesparan, and E. R. Villegas, "Performance-Power Consumption Trade-off in Wearable Epilepsy Monitoring Systems" IEEE Journal of Biomedical and Health Informatics, vol. 19, no. 3, pp 1019-1028, may 2015.
- [10] P. Swami, T. K. Gandhi, B. K. Panigrahi, M. Tripathi, and S. Anand, "A novel robust diagnostic model to detect seizures in electroencephalography", Article in Expert Systems with Applications, Elsevier, and pp 116-130, March 2016.
- [11] W. G. Besio, I. E. M. Juárez, O. Makeyev, J. N. Gaitanis, A. S. Blum, R. S. Fisher, and A. V. Medvedev, "High-Frequency Oscillations Recorded on the Scalp of Patients With Epilepsy Using Tripolar, Concentric Ring Electrodes", IEEE Journal of Translational Engineering in Health and Medicine, vol. 2, June 2014.
- [12] U. Jindal, M. Sood, A. Dutta, and S. Roy Chowdhury, "Development of Point of Care Testing Device for Neurovascular Coupling from Simultaneous Recording of EEG and NIRS During Anodal Transcranial Direct Current Stimulation", IEEE Journal of Translational Engineering in Health and Medicine, vol. 3, 2015.
- [13] A. Awad, R. Hussein, A. Mohamed and A. A. El-Sherif, "Energy-Aware Cross-Layer Optimization for EEG-based Wireless Monitoring Applications", proceedings of 38th Annual IEEE Conference on Local Computer Networks, pp 356-363, 2013.
- [14] A. K. Tiwari, R. B. Pachori, V. Kanhangad, and B. K. Panigrahi, "Automated Diagnosis of Epilepsy using Keypoint Based Local Binary Pattern of EEG Signals", IEEE Journal of Biomedical and Health Informatics, pp 1-10, July 2016.
- [15] B. J. Edelman, B. Baxter, and B. He, "EEG Source Imaging Enhances the Decoding of Complex Right-Hand Motor Imagery Tasks", IEEE Transactions on Biomedical Engineering, vol. 63, no. 1, pp 4-14, January 2016.
- [16] M. I. Khalid, T. Alotaiby, S. A. Aldosari, S. A. alshebeili, M. H. al-Hameed, F. S. Y. Almohammed, and T. Alotaibi "Epileptic MEG Spikes Detection Using Common Spatial Patterns and Linear Discriminant Analysis", IEEE Access, pp 4629-4634, September 2016.
- [17] L. Dominique, J. Fiederer, J. Lahr, J. Vorwerk, F. Lucka, A. Aertsen, C. H. Wolters, A. S. Bonhage, and T. Ball, "Electrical Stimulation of the Human Cerebral Cortex by Extracranial Muscle Activity: Effect Quantification With Intracranial EEG and FEM Simulations", IEEE Transactions on Biomedical Engineering, vol. 63, no. 12, pp 2552-2563, December 2016.
- [18] Y. Blokland, L. Spyrou, D. Thijssen, T. Eijssvogels, W. Colier, M. F. Westerdijk, R. Vlek, J. Bruhn, and J. Farquhar, "Combined EEG-fNIRS Decoding of Motor Attempt and Imagery for Brain Switch Control: An Offline Study in Patients With Tetraplegia" IEEE Transactions on Neural Systems and Rehabilitation Engineering, vol. 22, no. 2, pp 222-229, March 2014.
- [19] A. V. Luhmann, H. Wabnitz, T. Sander and K. R. Muller, "M3BA: A Mobile, Modular, Multimodal Biosignal Acquisition architecture for miniaturized EEG-NIRS based hybrid BCI and monitoring", IEEE Transactions on biomedical engineering, pp 1-12, July, 2016.
- [20] W. V. Rosenberg, T. Chanwimalueang, V. Goverdovsky, D. Looney, D. Sharp, and D. P. Mandic, "Smart Helmet: Wearable Multichannel ECG and EEG", IEEE Journal of Translational Engineering in Health and Medicine, vol.4, pp 1-12, November 2016.

BIOGRAPHIES



Engineering in Electrical Engineering in 2008 from PEC

Mr. Anurag Verma is working as Assistant Professor in Department of EEE of NIET, Greater Noida. He graduated from the Dayalbagh Educational Institute, (DU) Agra in 2003 in Electrical Engineering and completed his Master of



University of Technology (DU), Chandigarh and presently pursuing his Ph.D. from Dayalbagh Educational Institute, (DU) Agra. He is life member of Systems society of India and an active member of IEEE from 2012 to 2015. He published six papers in national and international conferences and three journal papers so far in the field of Renewable energy systems, intelligent computing systems, soft computing and power electronics. He has five years of Industrial experience in Garg Electronics, Panchkula, Haryana for PCB prototyping.

Prof. Laxman Singh obtained his B. Tech in Electronics and Communication Engineering and M.Tech in Instrumentation and Control from M.D. University, Haryana, India in 2004 and 2009 respectively. He obtained his PhD degree from Jamia Millia Islamia (a central Govt. of India University) in 2016. Presently he is working as Associate Professor in the Department of Electronics & Communication Engineering in Noida Institute of Engineering & Technology (NIET), Greater Noida. Dr. Laxman Singh has published many research papers in the area of Electronics and Communication Engineering in refereed international /national journals and conferences. His current research interests are in the areas of wavelet analysis, neural network, and image processing.



Mr. M. Hari: He is working as Assistant Professor in Department of EEE of NIET, Greater Noida. He had received his Bachelor degree in Electrical and Electronics Engineering from MITS College, Madanapalle in 2013, and had his Postgraduate in Power Electronics from SITAMS (Autonomous) college, Chittoor, AP.